Life Model of Hollow Cathodes Using a Barium Calcium Aluminate Impregnated Tungsten Emitter*†

S. D. Kovaleski
QSS Group, Inc.
NASA Glenn Research Center Group
21000 Brookpark Rd.
Cleveland, OH 44135
216-433-3735
scott.kovaleski@grc.nasa.gov

IEPC-01-276

Hollow cathodes with barium calcium aluminate impregnated tungsten emitters for thermionic emission are widely used in electric propulsion. These high current, low power cathodes are employed in ion thrusters, Hall thrusters, and on the International Space Station in plasma contactors. The requirements on hollow cathode life are growing more stringent with the increasing use of electric propulsion technology. The life limiting mechanism that determines the entitlement lifetime of a barium impregnated thermionic emission cathode is the evolution and transport of barium away from the emitter surface. A model is being developed to study the process of barium transport and loss from the emitter insert in hollow cathodes. The model accounts for the production of barium through analysis of the relevant impregnate chemistry. Transport of barium through the approximately static gas is also being treated. Finally, the effect of temperature gradients within the cathode are considered.

Introduction

Hollow cathodes find extensive use in electric propulsion. Hollow cathodes are used in ion thrusters and Hall thrusters [1] to provide electrons for both propellant ionization and neutralization. International Space Station plasma contactors [2] use hollow cathodes to emit electron current, as demanded, to the ambient space plasma at low coupling voltages, thus compensating for spacecraft charging. For all of these applications, long cathode lifetime is critically important.

The entitlement, or theoretical maximum, lifetime of the cathode is dependent upon the chemistry of the oxide impregnated tungsten emitter insert. The cathode insert serves as a low work function thermionic electron source for internal ionization of the cathode expellant [1]. The tungsten emitter work function is lowered by a surface coating of barium on oxygen on tungsten [3]. Barium is supplied to the tungsten surface by chemical reactions of the $BaO:CaO:Al_2O_3$ mixture with which the porous tungsten emitter is impregnated. In addition to supplying barium, products of the impregnate reactions will clog the emitter pores impeding the progress of barium to the surface. The impregnate can also react with impurities to produce "poisons" on the emitter surface. These "poisons" can increase the surface work function by displacing the barium-on-oxygen monolayer. Thus, it is apparent that an understanding of the chemistry of the impregnate is critically important.

The $BaO:CaO:Al_2O_3$ impregnated tungsten cathodes have been widely studied since their development by Levi [4]. Common cathode impregnate compositions include 5:3:2, 4:1:1 and 3:1:1, where the notation indicates the stoichiometric coefficient of BaO: CaO: Al_2O_3 [5]. The chemistry of operation of impregnated cathodes was studied originally by Rittner, Rutledge,

* Presented as Paper IEPC-01-276 at the 27th International Electric Propulsion Conference, Pasadena, CA, 15-19 October, 2001.

and Ahlert [6]. The chemistry of barium aluminate impregnates with added CaO were examined by Rittner [7]. Suitch examined the thermochemistry and kinetics of barium aluminate and barium calcium aluminate compounds in detail [8]. Lipeles and Kan generalized a thermochemical model for the operation of impregnated cathodes [9], and it is upon their work that the model reported here is based.

Sarver-Verhey reported experimental results of a xenon hollow cathode destructive analysis, after 28,000 hours of cathode operation [10]. The results indicated significant chemical evolution of the emitter at fixed operating conditions had resulted in cathode failure. The results indicated that cathode electron emission was sustained only at the downstream end of the emitter. Depositions of $BaWO_4$ and Ba_2CaWO_6 were found on the surface of the upstream 70% of the emitter. Ample amounts of barium were found within the emitter, indicating that either the cathode was no longer able to create free barium due to progression of the internal chemical reactions, or that the surface of the cathode had been poisoned by tungstate formation. The results of these experiments shed new light on the end-of-life mechanisms of the impregnated emitters used on xenon hollow cathodes.

In light of the results of Sarver-Verhey's experiments, and in order to support continuing effort to improve the lifetime of ion thruster and plasma contactor cathodes, a need for a better understanding of the life limiting chemical phenomena in xenon hollow cathodes was identified. The models of cathode operation presented above were usually applied to cathodes used in vacuum tubes. Gaseous products evolved from these cathodes freely expand into vacuum. The situation in a xenon hollow cathode is quite different, where a few Torr of xenon is present over the emitter, impeding transport of gaseous products away from the surface and encouraging additional reactions at the emitter surface. Significant temperature gradients are also present in hollow cathodes that are not present in other dispenser cathode applications. For these reasons, a thermochemical model of the emitter coupled to a diffusion model of gas phase transport within a hollow cathode has been developed. The model includes a dependence on empirically derived cathode emitter temperature profiles. In this way, a simple analysis of the chemical processes within hollow cathodes has been performed.

Model Description

The orificed hollow cathode, used extensively in electric propulsion technology and in the International Space Station plasma contactor, is the device this model attempts to describe. Orificed hollow cathodes are characterized by a refractory metal tube through which an inert gas flows. At the downstream end of the tube, a small diameter orifice is employed to reduce the cathode gas flow necessary for low voltage cathode operation by increasing the internal pressure. These hollow cathodes generally use a porous tungsten emitter impregnated with work function lowering barium calcium aluminate to generate an internal plasma. A diagram of an orificed hollow cathode is shown in figure 1.

The model of orificed hollow cathodes that has been developed couples a thermodynamic model of the barium calcium aluminate chemical system with a diffusion model to estimate the barium supply and loss rates in the cathode. Empirical transfer functions are used by the model to estimate the hollow cathode internal pressure and emitter temperature profile based on discharge current, orifice diameter, and gas flow rate. The emitter temperature profile then serves as an input to the thermochemistry model to determine the partial pressures of gaseous barium and barium oxide within the emitter pores. The partial pressures in the interior of the emitter pores and the partial pressure in the interior of the cathode determines the rate of free molecular flow of barium and barium oxide gas out of the emitter. Diffusion through the inert gas flowing through the cathode determines rate of loss of barium and barium oxide leaving the cathode orifice and diffusing upstream of the cathode.

The use of thermodynamically derived gaseous Ba and BaO partial pressures to estimate free molecular flow rates from the emitter pores implies that the applicable reaction rates in the emitter are fast compared to the rates of loss from the emitter pores. The use of a thermochemical approach should at a minimum provide an upper bound on the loss rate of Ba and BaO from the emitter, and may be quite accurate given the small reaction volumes within the emitter pores and long residence times of the diffusing Ba and BaO gas. As long as the time rate of change of critical parameters like composition and partial pressure of Ba and BaO are slower than the characteristic time of reaction kinetics, this thermodynamic approach should

be a good one. The model also implies that other supply mechanisms of Ba and O to the cathode surface, like surface diffusion along the pore walls, are small.

Thermochemistry model

The thermodynamic model of the barium calcium aluminate impregnated tungsten emitter used here was first reported by Lipeles and Kan [9]. The model starts with the assumption that first, gaseous BaO is formed by thermal decomposition of the impregnate materials. Barium gas is then formed by reduction of gaseous BaO by tungsten according to the reaction,

$$2BaO(g) + \tfrac{1}{3}W(s) \leftrightarrow \tfrac{1}{3}Ba_3WO_6(s) + Ba(g). \qquad (1)$$

If the partial pressure of BaO is known, the barium vapor pressure can be calculated from the equilibrium constant of Equation 1,

$$p_{Ba} = p_{BaO}^2 * K_{eq} = p_{BaO}^2 \exp\left(-\tfrac{\Delta H}{RT} + \tfrac{\Delta S}{R}\right), \qquad (2)$$

where $p_{Ba}=P_{Ba}/P_{\text{std}}$ signifies a pressure of barium relative to standard pressure, and p_{BaO} has a similar definition. The equilibrium constant is given by the exponential; the arguments of the exponential, *DH* and *DS*, are the enthalpy and entropy of reaction, respectively.

Barium oxide gas is produced by the thermal decomposition of the barium-containing phases of the impregnate material. The phase with the largest partial pressure of gaseous BaO will determine the vapor pressure of BaO above the impregnate. The vapor pressures of BaO produced by the thermal decomposition of pure phases are calculated using the equation

$$p_{BaO} = \frac{P_{BaO}}{P_{std}} = \exp\left(-\tfrac{\Delta H}{RT} + \tfrac{\Delta S}{R}\right), \qquad (3)$$

where the definition of the variables are analogous to those of equation 2. The thermodynamic constants, *DH* and *DS*, for the reactions used by this model were tabulated by Lipeles and Kan or were calculated by the method of Lipeles and Kan [9].

The phase composition of the impregnate determines which thermal decomposition reactions are potentially active in the production of BaO gas. For a given stoichiometric composition of the impregnate, the phase composition is determined from the BaO-CaO-Al_2O_3 phase diagram [11]. The relative molar percentages of BaO, CaO, and Al_2O_3 in the impregnate are determined, and the position of the impregnate on the diagram is found. The relative molar amounts of the constituent phases are then determined by the lever rule, as described in [9]. The thermal decomposition reaction of each phase is assessed for the partial pressure of barium oxide it produces. For compositions consisting of three pure phases, the partial pressures above the phases are calculated from equation 3. For compositions consisting of two phases, either a pure phase in equilibrium with a solid solution or two solid solutions in equilibrium, the solid solutions are assumed to be ideal. The vapor pressure above an ideal solution is the sum of the vapor pressures of the component pure phases weighted by the mole fractions of each pure phase in the solution. Thus the vapor pressure above a solid solution is given by

$$P_{SS} = X_1 P_1 + X_2 P_2, \qquad (4)$$

where X_1 and X_2 are the mole fraction of phase 1 and 2 and $X_1 + X_2 = 1$. Once the vapor pressure above each phase present, either pure phase or solid solution, is calculated, the vapor pressures are compared. The phase with the highest vapor pressure of gaseous BaO is the active phase. It will produce BaO and suppress the other decomposition reactions.

The supply of gaseous BaO and Ba from the interior of the emitter pores to the interior volume of the hollow cathode was modeled as free molecular flow. Assuming cylindrical pores on a typical cathode emitter, the pore area is ~20 μm^2, and the pore diameter is then ~5 μm. The mean free path of a barium atom or barium oxide molecule in 10 Torr of Xe gas is about 20 μm. Thus, since the mean free path is approximately 4 times larger than the pore diameter, free molecular flow was assumed to be a relatively valid model for gaseous species escape through the emitter pores. Note that, for this model, only the inward-facing surface of the emitter cylinder was assumed to supply gaseous species. Supply from the surface facing the cathode tube wall was neglected. The mass flow rate out of a pore is given by

$$\dot{m}_{out} = A_{pore}\sqrt{\frac{M}{2pR}}\left(\frac{P_{insert}}{\sqrt{T_{insert}}} - \frac{P_{cathode}}{\sqrt{T_{gas}}}\right), \qquad (5)$$

where A_{pore} is the cross-sectional area of the pore, M is the molecular mass of the gas, P_{insert} and T_{insert} are the pressure and temperature of the gas within the emitter pore, and $P_{cathode}$ and T_{gas} are the temperature and pressure of the gas in the cathode interior. For the purposes of this model, the emitter temperature was calculated using transfer functions derived from the data of Salhi [12]. The data in Table 1, taken from [12], were fit by multiple linear reqression to generate the transfer function for emitter temperature. The pressures of gaseous species within the emitter pores were calculated by Equations 2 and 3. The gas temperature, both within the emitter pores and within the cathode interior volume, was assumed to be approximately equal to the emitter temperature. The pressure of gaseous species in the cathode interior was determined using a simple one-dimensional diffusion model of the cathode.

Diffusion model

A simple, steady-state, one-dimensional diffusion model with advection was used to estimate the loss of Ba and BaO gas from the interior of the cathode. In 10 Torr of Xe at 1373 K, the mean free path of Ba is approximately 20 μm. Thus, the mean free path is much smaller than the 6.35 mm diameter cathode tube. For a 7 sccm flow rate of Xe gas at 1373 K and 10 Torr, the gas velocity in the interior of a 0.25 inch diameter cathode is 4 m/s. Given this velocity, the advective flux is estimated to be an order of magnitude greater than the diffusion flux, requiring inclusion of the advection term. Since the velocity is derived from a regulated Xe flow, and since the source of Ba and BaO varies relatively slowly with time, a steady-state model was employed.

A schematic of the cathode diffusion model is shown in figure 2. The loss of Ba and BaO through the cathode orifice was approximated as the flow rate of Xe through the orifice times the mole fraction of Ba or BaO in the Xe. Ba and BaO were assumed to condense on the cathode tube upstream of the emitter. Using a thermodynamic equation analogous to Equation 3 for the vapor pressure of either Ba or BaO above a surface at temperature T and the ideal gas law, a density gradient could be related to the temperature gradient along the surface. Thus, the diffusion flux at the upstream end of the emitter was given by

$$-D\left.\frac{dn}{dx}\right|_{x=L} = \frac{-Dn}{T}\left[\frac{\Delta H_{evap}}{RT} - 1\right]\left.\frac{dT}{dx}\right|_{x=L}, \qquad (6)$$

where D is the diffusion coefficient, n is the gaseous species density, T is the cathode tube surface temperature, DH_{evap} is the heat of evaporation, and L denotes the upstream end of the emitter insert. All gradients and spatially dependent variables are evaluated at the upstream end of the emitter. Ba and BaO gas release from the pores on the emitter surface into the cathode interior was approximately treated as generation within the cathode volume. The diffusion equation was solved by the finite difference method.

Thermochemistry and diffusion model solution

The thermochemistry and diffusion models are solved serially and then repeated to march the solution through time. Initially the cathode current, orifice diameter, flow rate, pore count and emitter density, and emitter dimensions are input. In addition, the relative molar percentages of BaO, CaO, and Al_2O_3 in the impregnate are given. Next, the cathode internal pressure and emitter temperature profile are calculated from transfer functions derived from the data of Salhi [12]. The Xe pressure is used to calculate the diffusion coefficient. The emitter temperature and impregnate composition are fed into the thermochemistry model. The impregnate stoichiometric composition is applied to the BaO-CaO-Al_2O_3 phase diagram to determine the impregnate phase composition. The partial pressure of BaO above each phase is determined from the decomposition reaction equilibrium constant. The phase with the largest partial pressure is assumed to be the active phase, and the BaO pressure is set to the partial pressure of its decomposition reaction. This pressure is then used in equation 2 to determine the pressure of gaseous Ba in the emitter pores. Given the pressure inside the emitter pores, the diffusion model can be self-consistently solved to calculate the Ba and BaO gas densities within the cathode. In addition, the flow rate of gaseous Ba and BaO into or out of the emitter pores is calculated. From the flow rate, the amount of Ba and BaO lost from or gained by the emitter can be calculated, and a new impregnate composition is computed. The time step is indexed, and the solution

is repeated. In this manner, the model is stepped through time, to the specified end point.

Model Results

Since the emitter temperatures and cathode internal pressures are derived from an empirical expression, unless otherwise noted, model results are for a cathode geometry set to match that of Salhi [12]. As such, the modeled cathode inner diameter was 5.32 mm, the emitter inner diameter was 3.8 mm, and the emitter length was 25.4 mm. Cathode currents were allowed to vary between 1 and 10 A, xenon flow rates could vary from 7 to 13 sccm, and cathode orifice diameters could range from 1.2 to 2.0 mm. Except for the NSTAR cases, cathode current was 3.0 A, the flow rate was 7 sccm, and the orifice diameter was 1.2 mm.

For the initial runs of this hollow cathode emitter chemistry model, an emitter initial composition of 4BaO: CaO: Al_2O_3 was modeled. This composition falls in a three phase region of the phase diagram and is composed of BaO, CaO, and $Ba_{3.74}Ca_{0.26}Al_2O_7$. Figure 3 shows the partial pressures as a function of temperature of the barium containing species of the impregnate. The thermal decomposition of BaO is the highest vapor pressure reaction, and will therefore be the dominant reaction of the impregnate initially. As the BaO is depleted, the impregnate composition will cross into a two phase region, with CaO in equilibrium with a solid solution varying in composition between $Ba_{3.74}Ca_{0.26}Al_2O_7$ and $Ba_{3.508}Ca_{0.492}Al_2O_7$. The BaO vapor pressure from the thermal decomposition reaction of both of these compounds is similar to that of $Ba_{3.74}Ca_{0.26}Al_2O_7$. The thermal decomposition of the solid solution is the dominant reaction in this region. The vapor pressure will range between the vapor pressures of the two pure phases determined by the mole fraction of each in the solid solution, as given by Equation 4. The vapor pressure of BaO above both compounds is much lower than that above solid BaO, as can be seen in Figure 3. As a consequence, the loss rate of Ba from the emitter drops precipitously once the boundary between the three and two phase regions is passed.

The effect of this sharp drop in BaO pressure is seen in the loss rates of Ba and BaO from the modeled cathode after 2000 model hours of operation. Figure 4 shows the rate at which Ba and BaO are lost from and returned to the emitter as a function of axial position relative to the orifice plate. Note the sharp drop in loss rate between the orifice at 0 mm and approximately 12 mm. In the portions of the cathode emitter close to the orifice, the temperatures are higher and consequently the Ba and BaO pressures within the emitter are higher. This increases the rate gaseous species exit the emitter pores. Thus, the BaO content of the impregnate in the downstream region is more quickly depleted than the upstream region. Eventually the impregnate composition is such that a new region on the phase diagram is entered. The pressure of Ba and BaO gas then drops precipitously. If the partial pressure of Ba and BaO in the cathode, but exterior to the emitter, is large enough, the process is reversed and BaO is returned to the emitter. This is seen in figure 4 between 9 and 13 mm from the orifice plate, where the return rate exceeds the loss rate.

As mentioned above, the largest change in the Ba content of the impregnate occurs in the downstream sections of the emitter. Figure 5 shows the fraction of BaO lost from the emitter as a function of position and time. Examining figure 5, a steep composition gradient is observed in the first few millimeters of the emitter early in time. Upstream of the gradient (toward positions further from the orifice), the composition of the emitter remains relatively unchanged. Downstream of the gradient (toward positions nearer the orifice), significant amounts of BaO have been lost. This steep gradient moves upstream with time, but decelerates as cooler regions of the emitter begin contributing to the loss of BaO. The BaO lost from the emitter enters the cathode interior as gaseous BaO or as gaseous Ba. From the gas phase, it is available for deposition on the insert surface for work function lowering.

To assess the differences between cathodes operated under different conditions, two NSTAR-like cases were compared. The NSTAR discharge cathode at throttle level TH0, or minimum power, and at TH15, or maximum power, was modeled though 10,000 hours of operation [13]. The temperature distribution and cathode internal pressure calculations were modified from that of [12] to more accurately represent the NSTAR cathode. Figure 6 compares the fraction of BaO lost from the emitter insert after 10,000 model hours of running at conditions simulating the TH0 and TH15 operating points. After 10,000 hours of operation at TH15, the model predicts up to 90% of the BaO originally present in the

downstream end of the emitter has been depleted. By comparision, at most 16% of the BaO is depleted in 10,000 model hours at TH0. This difference is likely due to the increased operating temperature of the cathode at TH15.

Assuming the barium responsible for lowering the emitter work function is deposited from the gas phase barium in the cathode interior, the axial barium density in the cathode should be related to cathode performance. Examination of Figure 7 shows that the barium density in the TH15 cathode is still at least one order of magnitude higher than the barium density within the TH0 cathode at the downstream end. So even though the fraction of barium lost from the emitter is larger for the TH15 cathode, it is still expected to have ample gas phase Ba available to lower the emitter work function.

An interesting difference is noted when a modeled cathode run for 8,000 hours at TH15 is compared to a modeled cathode run for 8,000 hours at TH0. When both cathodes are compared at TH0 after 8,000 hours at different conditions, Figure 8 shows that the gaseous Ba density is different for these two cathodes. At the downstream end of the cathode, where work function lowering is most important, the cathode run at TH0 for 8,000 hours has a barium density 4 times higher than its counterpart run at TH15. Compositional differences arise due to the difference in cathode operating power, which results in lower densities when the cathodes are subsequently compared at the same power. The compositional differences result in differing decomposition reactions between the two cathodes, which in turn results in different Ba supply rates. The gas phase Ba density difference could affect the performance of cathodes operated at low power, which were run previously at high power for extended periods. These results suggest that cathode operating-power history also affects cathode life and operability.

Conclusions

A coupled thermochemistry/diffusion model has been developed for xenon hollow cathode operation that shows good qualitative agreement with observable phenomena in hollow cathodes. The thermochemical model from Lipeles and Kan [9] has been used to estimate the supply of gaseous Ba and BaO from the impregnated tungsten emitter. This supply is coupled to a simple, one-dimensional diffusion model of the cathode to examine the transport of these gases through the xenon gas flowing through the cathode. The model has been used initially to examine the evolution and loss of Ba from the emitter impregnate. Model results at differing cathode power levels have also been compared.

Several key results have been found during the inaugural model runs. The effect of emitter composition on the supply of Ba and BaO gas to the interior of the cathode has been quantified. The higher temperature downstream region of the emitter, near the orifice, has been shown to be most active in the production of Ba and BaO. The fraction of barium lost from the emitter is largest near its downstream end. The region of BaO loss moves upstream with time, decelerating as cooler regions of the emitter are reached.

An NSTAR-like cathode operated at TH15 and TH0 was also modeled. The fraction of BaO lost from the modeled cathode run for 10,000 model hours at TH15 was shown to be much greater than the cathode run at TH0. This was attributed to the higher operating temperature of the cathode at TH15. In spite of its compositional differences, the cathode run at TH15 was shown to produce more gaseous Ba than the TH0 cathode. By contrast, after 8,000 hours of operation, a lower Ba density was produced internally in a cathode run at TH15 compared to a cathode run at TH0, when both were compared at TH0. The lower Ba density was due to differences in the emitter chemistry between the two cathodes. This suggested that the history of cathode operating power could be a significant parameter in determining useful cathode life.

References

[1]. Kaufman, H.R., "Technology of Electron Bombardment Ion Thrusters," *Advances in Electronics and Electron Physics*, vol. 36, New York: Academic Press, Inc., 1974.

[2]. Patterson, M.J., et al., "Space Station Cathode Design, Performance, and Operating Specifications," *25th International Electric Propulsion Conference Proceedings*, IEPC Paper No. 97-170, August 24-28, 1997.

[3]. Springer, R.W., Haas, T.W., "Auger Electron Spectroscopy Study of Cathode Surfaces During Activation and Poisoning I. The Barium-on-Oxygen-on-Tungsten Dispenser Cathode," *J. Appl. Phys.* ***45****, 5260-5263,* December 1974.

[4]. R. Levi, "Improved "Impregnated Cathode"," *J. Appl. Phys.* ***26****, 639*, May 1955.

[5]. Cronin, J.L., "Modern Dispenser Cathodes," *IEE Proc.* ***128****, 19-32,* February 1981.

[6]. Rittner, E.S., Rutledge, W.C., Ahlert, R.H., "On the Mechanism of Operation of the Barium Aluminate Impregnated Cathode," *J. Appl. Phys.* ***28****, 1468-1473*, December 1957.

[7]. Rittner, E.S., "On the Mechanism of Operation of the Type B Impregnated Cathode," *J. Appl. Phys.* ***48****, 4344-4346*, October 1977.

[8]. Suitch, P.R., Doctoral Dissertation, Georgia Institute of Technology, Atlanta, Georgia, 1987.

[9]. Lipeles, R.A., Kan, H.K.A., "Chemical Stability of Barium Calcium Aluminate Dispenser Cathode Impregnants," *Appl. Surf. Sci.* ***16****, 189-206*, 1983.

[10]. Sarver-Verhey, T.R., "Destructive Evaluation of a Xenon Hollow Cathode After a 28,000 Hour Life Test", *34th AIAA/ASME/SAE/ASEE Joint Propulsion Conference and Exhibit Proceedings*, AIAA Paper No. 98-3482, July 13-15, 1998.

[11]. Wolten, G.M., "An Appraisal of the Ternary System BaO-CaO-Al_2O_3", SD-TR-80-67, Space Division, Air Force Systems Command, Los Angeles, California, October, 1980.

[12]. Salhi, A., Doctoral Dissertation, The Ohio State University, Columbus, Ohio, 1993.

[13]. Rawlin, V.K., et al., "NSTAR Flight Thruster Qualification Testing," *34th AIAA/ASME/SAE/ASEE Joint Propulsion Conference Proceedings,* AIAA Paper No. 98-3936, July 13-15, 1998.

[14]. Soulas, G.C., "Multiple Hollow Cathode Wear Testing for the Space Station Plasma Contactor", *30th AIAA/ASME/SAE/ASEE Joint Propulsion Conference Proceedings*, AIAA Paper No. 94-3310, June 27-29, 1994.

Table 1. Data taken from [12] to generate a transfer function for emitter insert temperature as a function of position, discharge current, and orifice diameter. Values in parentheses are interpolated values.

Emitter Insert Temperature Profile (K)					
Orifice Diam. = 1.21 mm		Distance from Orifice (mm)			
		1	6	16	25
Discharge Current (A)	10	1328	(1268)	1149	1075
	7	1259	(1203)	1092	1020
	4	1178	(1127)	1025	955
	2	1117	(1066)	963	896
Orifice Diam. = 0.76 mm		Distance from Orifice (mm)			
		3	6	13	22
Discharge Current (A)	10	1342	1232	(1160)	987
	7	1291	1188	1101	967
	4	1247	1152	1077	944
	2	1160	1079	1009	865

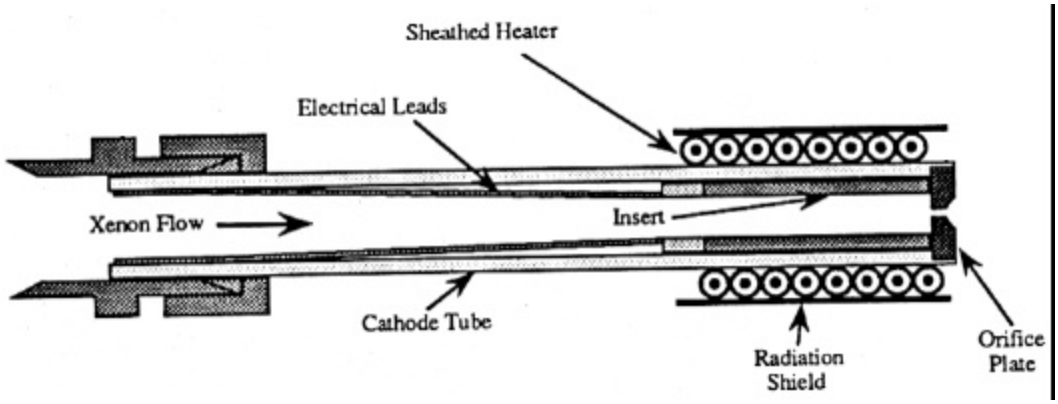

Figure 1. Diagram of a xenon hollow cathode (drawing not to scale) [14]. The direction of xenon flow is indicated.

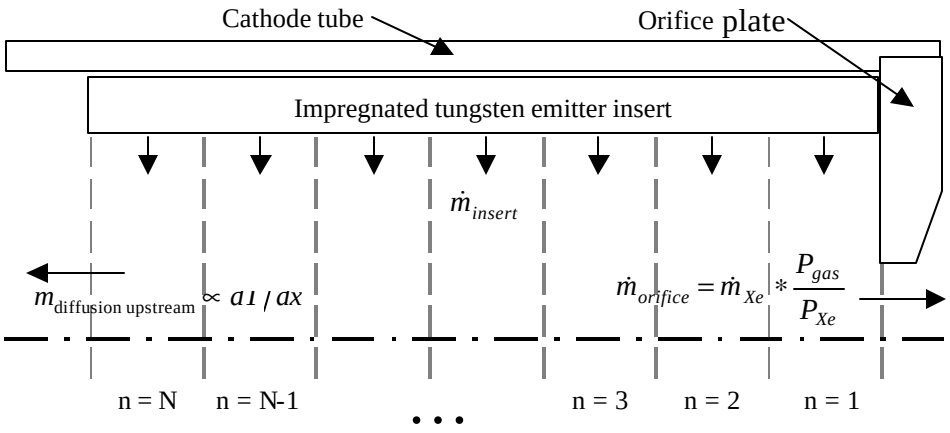

Figure 2. Schematic diagram of the hollow cathode diffusion model. The slices indicate slices of the 1-D diffusion model. Upstream and downstream boundary conditions are indicated. Ba or BaO gas supply from the emitter insert is treated as volume generation within a slice.

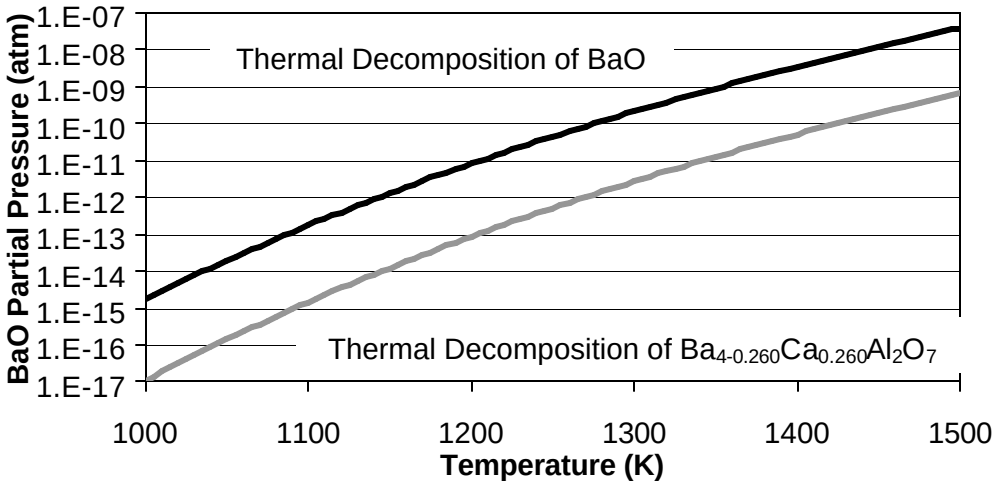

Figure 3. Partial pressure of gaseous BaO for the thermal decomposition of pure BaO and of a $Ba_4Al_2O_7$ with substitutional Ca. These are the phases in 4:1:1 dispenser cathode impregnates active in production of gaseous BaO.

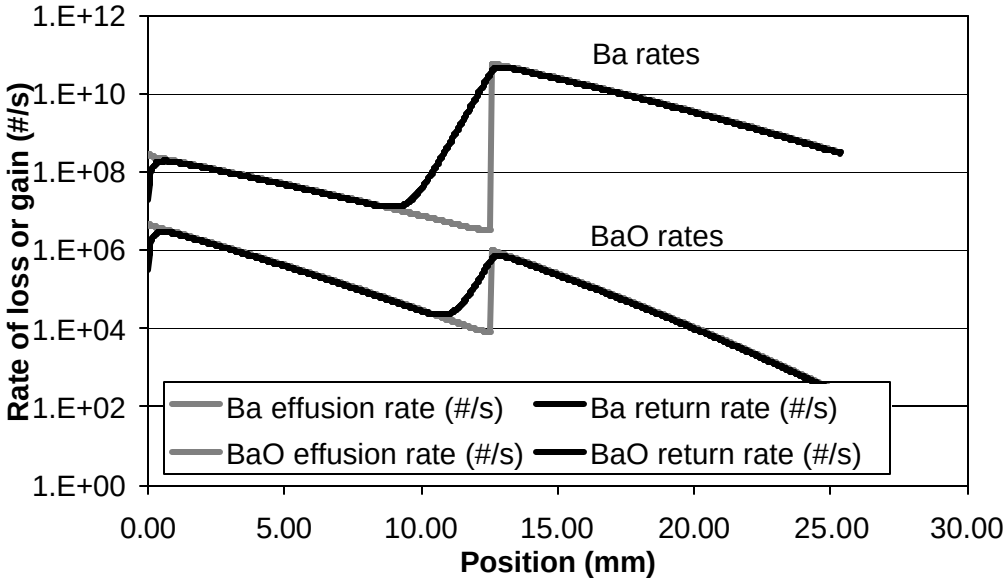

Figure 4. Rate of outward flow of Ba or BaO from the emitter or rate of return of those gases back to the emitter after 2000 hours of model operation. Rates stated in number per second. Discontinuity in outward flow rate is due to a localized phase change after loss of BaO from the impregnate. Dominant BaO producing phase changes from a high vapor pressure phase to a low vapor pressure phase.

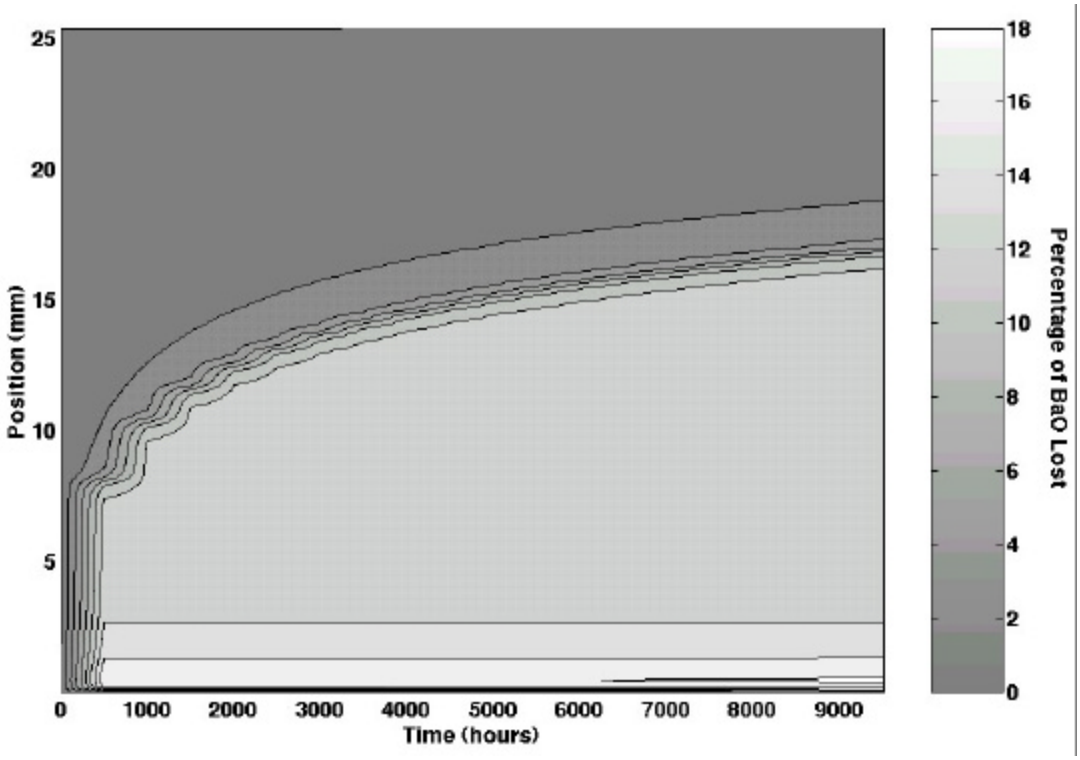

Figure 5. Fraction of the original barium oxide lost from the emitter over 9500 model hours. The color key indicates the fraction, with gray representing zero barium oxide lost and white representing 18% barium oxide lost.

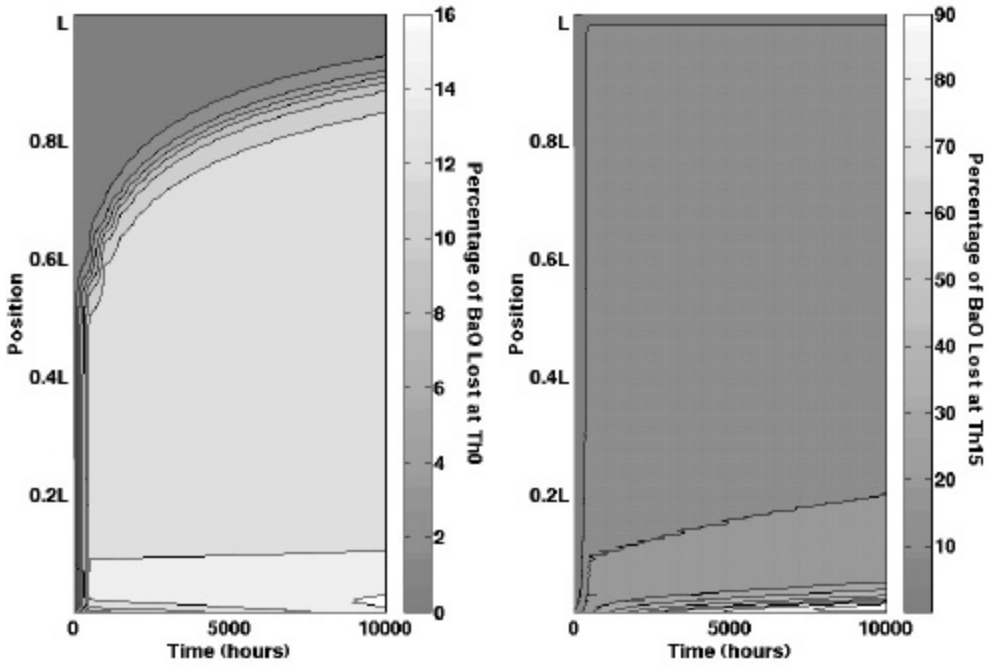

Figure 6. Comparison of BaO loss from the emitter insert of an NSTAR-like discharge cathode modeled at throttle levels TH0 and TH15. Cathode operation over 10,000 hours at each throttle level was modeled. Color keys to the right of each contour plot indicate the percentage of BaO lost. Position given relative to L, which represents the NSTAR emitter insert length.

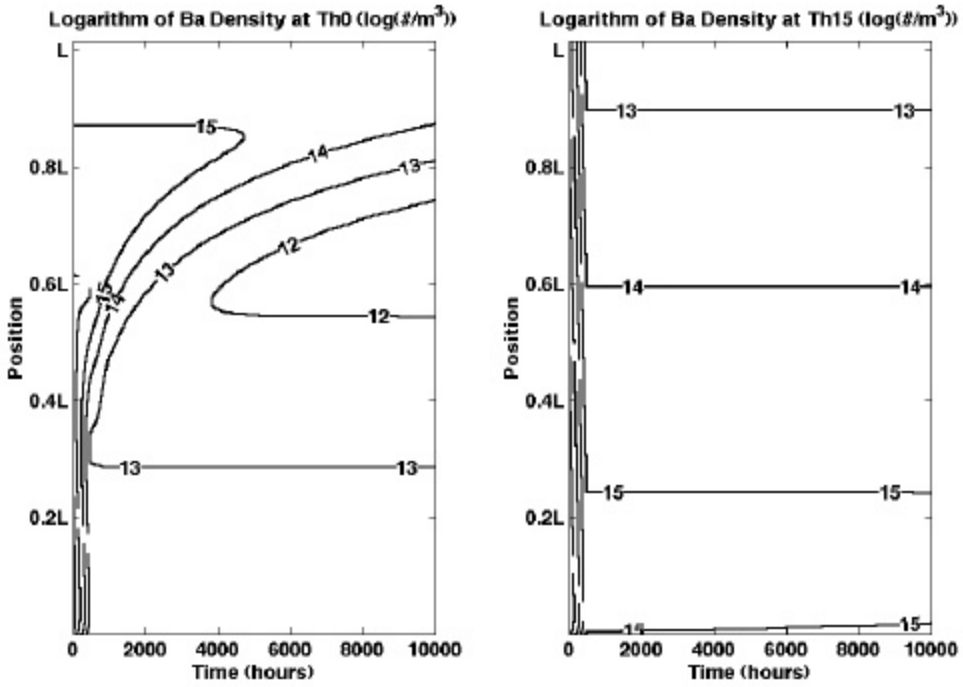

Figure 7. Comparison of gaseous Ba density in the interior of an NSTAR-like discharge cathode modeled at throttle levels TH0 and TH15. Cathode operation over 10,000 hours at each throttle level was modeled. Position given relative to L, which represents the NSTAR emitter insert length.

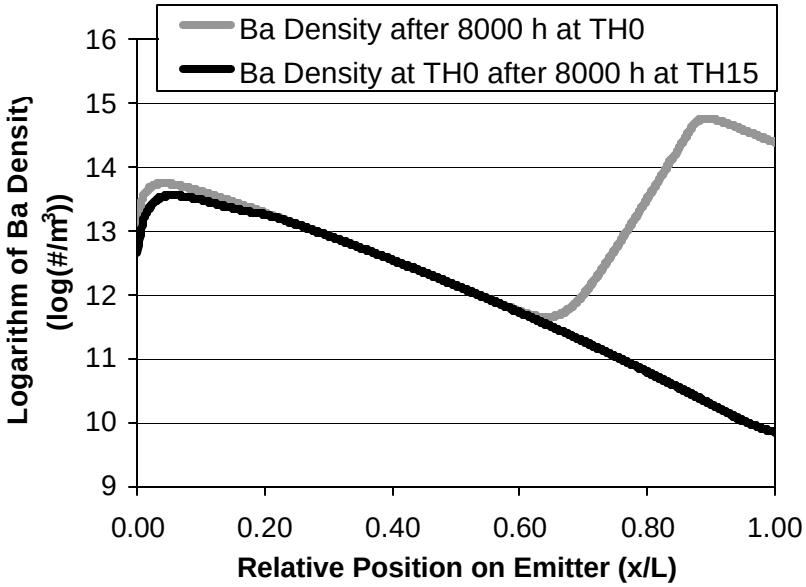

Figure 8. Comparison of gaseous Ba density in the interior of an NSTAR-like discharge cathode modeled at throttle levels TH0 and TH15. Ba densities are produced at TH0 for both cathodes, after 8000 hours of operation at their individual operating points. Position given relative to L, which represents the NSTAR emitter insert length.